

UCLA

UCLA Previously Published Works

Title

Earlier Detection of Glaucoma Progression Using High-Density 3-Dimensional Spectral-Domain OCT Optic Nerve Volume Scans

Permalink

<https://escholarship.org/uc/item/6hg9h5sw>

Journal

Ophthalmology Glaucoma, 4(6)

ISSN

2589-4234

Authors

Ratanawongphaibul, Kitiya
Tsikata, Edem
Zemplenyi, Michele
[et al.](#)

Publication Date

2021-11-01

DOI

10.1016/j.ogla.2021.03.010

Peer reviewed



HHS Public Access

Author manuscript

Ophthalmol Glaucoma. Author manuscript; available in PMC 2022 November 01.

Published in final edited form as:

Ophthalmol Glaucoma. 2021 ; 4(6): 604–616. doi:10.1016/j.ogla.2021.03.010.

Earlier Detection of Glaucoma Progression Using High-Density 3D Spectral-Domain Optical Coherence Tomography Optic Nerve Volume Scans

Kitiya Ratanawongphaibul, MD^{1,2,3}, Edem Tsikata, PhD^{1,2}, Michele Zemlenyi, PhD⁴, Hang Lee, PhD^{2,5}, Milica A. Margeta, MD, PhD^{1,2}, Courtney L. Ondeck, MD, MPhil^{1,2,6}, Janice Kim, MD², Billy X. Pan, MD^{1,2,7}, Paul Petrakos, DO, MS^{1,2,8}, Anne L. Coleman, MD, PhD⁹, Fei Yu, PhD^{9,10}, Johannes F. de Boer, PhD¹¹, Teresa C. Chen, MD^{1,2}

¹Department of Ophthalmology, Glaucoma Service, Massachusetts Eye and Ear, Boston, Massachusetts, United States

²Harvard Medical School, Boston, Massachusetts, United States

³Glaucoma Research Unit, Faculty of Medicine, Chulalongkorn University and King Chulalongkorn Memorial Hospital, Thai Red Cross Society, Bangkok, Thailand

⁴Department of Biostatistics, Harvard T.H. Chan School of Public Health, Boston, Massachusetts, United States

⁵Massachusetts General Hospital Biostatistics Center, Department of Medicine, Massachusetts General Hospital, Boston, Massachusetts, United States

⁶Department of Ophthalmology, VA Boston Hospital, Boston, Massachusetts, United States

⁷Beverly Hills Institute of Ophthalmology, Beverly Hills, CA.

⁸Department of Ophthalmology, New York Presbyterian/Weill Cornell Medicine, NY, NY

⁹Department of Ophthalmology, Stein Eye Institute, University of California, Los Angeles, United States

¹⁰Department of Biostatistics, UCLA Fielding School of Public Health, Los Angeles, California, United States

¹¹LaserLaB Amsterdam, Department of Physics and Astronomy, Vrije Universiteit, Amsterdam, The Netherlands; Department of Ophthalmology, Vrije Universiteit Medical Center, Amsterdam, The Netherlands

Abstract

Correspondence: Teresa C. Chen, MD, Massachusetts Eye and Ear, Glaucoma Service, 243 Charles Street, Boston, MA 02114, Teresa_chen@meei.harvard.edu.

Publisher's Disclaimer: This is a PDF file of an unedited manuscript that has been accepted for publication. As a service to our customers we are providing this early version of the manuscript. The manuscript will undergo copyediting, typesetting, and review of the resulting proof before it is published in its final form. Please note that during the production process errors may be discovered which could affect the content, and all legal disclaimers that apply to the journal pertain.

Purpose: To compare onset times of glaucoma progression among different glaucoma tests: disc photography (DP), visual field (VF) testing, two-dimensional (2D) retinal nerve fiber layer (RNFL) thickness, and three-dimensional (3D) spectral-domain optical coherence tomography (SD-OCT) neuroretinal rim measurements.

Design: Prospective longitudinal cohort study

Participants: One hundred and twenty-four eyes of 124 open angle glaucoma patients

Methods: Over a 5-year period, 124 open angle glaucoma patients had yearly DP, VFs, SD-OCT RNFL thickness scans, and optic nerve volume scans (Spectralis, Heidelberg Engineering, Heidelberg, Germany), all performed on the same day. From high-density optic nerve volume scans, custom-built software calculated the minimum distance band (MDB) thickness, a 3D neuroretinal rim parameter. Patients were classified as glaucoma progressors or non-glaucoma progressors using event-based analysis. Progression by DP and VF occurred when 3 masked glaucoma specialists unanimously concurred. Progression by RNFL and MDB thickness occurred if there was change greater than test-retest variability. Kaplan-Meier curves were constructed to analyze time-to-progression data. Kappa coefficients were used to measure agreement of progressing eyes among modalities.

Main Outcome Measures: Time to glaucoma progression among all 4 modalities

Results: Global MDB thickness detected glaucoma progression in the highest percentage of eyes (52.4%) compared to DP (16.1%, $P<0.001$), and global RNFL thickness (15.3%, $P<0.001$) respectively. Global MDB thickness detected glaucoma progression earlier than either DP (23 versus 44 months; $P<0.001$) or global RNFL thickness (23 versus 33 months; $P<0.001$). Among MDB progressing eyes, 46.2% were simultaneously or later confirmed by other conventional modalities. Agreement of glaucoma progressing eyes for all 4 modalities in paired fashion were slight to fair ($k=0.095-0.300$).

Conclusion: High-density 3D SD-OCT neuroretinal rim measurements detected glaucoma progression approximately 1–2 years earlier compared to current clinically available structural tests (i.e. disc photos and 2D RNFL thickness measurements).

Précis:

High-density three-dimensional spectral domain OCT neuroretinal rim measurements can detect glaucoma progression 1 to 2 years earlier than current clinically available disc photography and spectral domain OCT retinal nerve fiber layer thickness measurements.

Keywords

spectral domain optical coherence tomography; neuroretinal rim; glaucoma progression; volume scans; optic nerve

INTRODUCTION

Early detection of nerve damage is the key to preventing vision loss from glaucoma, because early detection allows for earlier treatments for glaucoma, the leading cause of irreversible blindness worldwide. Currently, there are many modalities to help clinicians

determine glaucoma progression, i.e. disc photography, visual fields, and spectral-domain optical coherence tomography (SD-OCT) retinal nerve fiber layer (RNFL) thickness measurements.¹ However, the gold-standard test has not yet been established.¹⁻³ The sequential comparison of disc photographs is subjective and qualitative; therefore, this method has poor agreement even among glaucoma specialists and furthermore cannot be used to quantify the rates of progression.⁴⁻⁶ For visual field assessments, measurements are quantitative but rely on the subjective response of the patient and may be difficult to obtain for some patients.^{3,7,8} In contrast, two-dimensional (2D) SD-OCT RNFL thickness has the advantage of being both objective and quantitative, but its clinical utility is limited by the measurement floor effect⁹ as well as its high rate of artifacts.¹⁰ To maximize the potential of SD-OCT imaging for early glaucoma detection, the development of objective quantitative three-dimensional (3D) measurements is needed.¹¹⁻¹⁴

Cross-sectional studies have suggested that new high-density 3D SD-OCT optic nerve measurements provide objective quantitative metrics but may be the same or better than the most commonly used 2D RNFL thickness parameter for diagnosing glaucoma.¹¹⁻¹⁴ Specifically, the minimum distance band (MDB) thickness measures the neuroretinal rim in 3D space and is a high-density version of the low-density commercially available Bruch's membrane opening - minimum rim width (BMO-MRW).¹¹⁻¹⁴ The MDB is calculated from an optic nerve volume scan, and it represents the neuroretinal rim as a band of tissue, whose width is the shortest distance between the outer OCT-based disc border (i.e. retinal pigment epithelium/Bruch's membrane, RPE/BM) and the inner cup surface (i.e. internal limiting membrane, ILM).¹¹⁻¹³ In addition to providing objective quantitative neuroretinal rim thickness measurements,^{11,13} MDB thickness has good correlation with structural assessments (i.e. disc photography vertical cup-disc ratio, $R = -0.88$, $P = .0003$) and with functional assessments (i.e. visual field mean deviation, $R = 0.63$, $P = .009$ and pattern standard deviation, $R = -0.87$, $P = .0004$).¹⁴ Although cross-sectional studies have suggested that MDB neuroretinal rim thickness is able to distinguish between normal and glaucomatous eyes,¹¹⁻¹³ there are no longitudinal studies evaluating the role of MDB rim thickness measurements for detection of glaucoma progression.

There are notable differences between the commercially available low-density BMO-MRW rim measurement and high-density MDB rim thickness measurement, the latter of which may represent the full potential of SD-OCT for glaucoma care. Although preliminary studies suggest that these reference-plane-independent BMO-MRW and MDB thickness neuroretinal parameters are similar or better than the most commonly used RNFL thickness parameter,¹¹⁻¹³ MDB thickness measurements possibly maximize the potential of SD-OCT for many reasons. For one, MDB thickness uses a high-density 193-line raster scan protocol and is calculated based on 100 points at the disc border whereas BMO-MRW uses a low-density 24 radial scan protocol and is calculated based on 48 points at the disc border.¹² Secondly, the OCT disc margin for MDB thickness measurements is defined as the RPE/BM complex termination¹⁴ whereas the BMO-MRW uses BMO as the disc margin. The RPE/BM is a more reliable feature for disc margin determination than BMO, because the RPE and BMO cannot normally be distinguished in SD-OCT images, largely due to the limited axial resolution of the Spectralis OCT machine.^{12,15} For these reasons, we used

MDB thickness as a possibly more accurate biomarker than BMO-MRW for the longitudinal study design of this proposal.

The study was designed to evaluate open angle glaucoma patients over a 5-year follow-up period to determine which progresses first: disc photography, Humphrey visual field testing, RNFL thickness measurements, or MDB thickness (i.e. neuroretinal rim thickness in 3D space). We hypothesize that MDB neuroretinal rim thickness can detect glaucomatous damage prior to existing structural and functional testing that is currently used to determine glaucoma progression.

MATERIALS AND METHODS

Participants, Clinical Exams, and Study Protocol

The longitudinal SD-OCT Imaging Glaucoma study was approved by the Massachusetts Eye and Ear Institutional Review Board. Since 2009, 2,000 study subjects were recruited from the Massachusetts Eye and Ear Glaucoma Service. All included patients provided informed consent in accordance with the Declaration of Helsinki and the regulations of the Health Insurance Portability and Accountability Act. Complete eye examinations were performed by a glaucoma specialist (T.C.C.) that consisted of history, best-corrected visual acuity, refraction, Goldmann applanation tonometry, slit-lamp biomicroscopy, gonioscopy, dilated ophthalmoscopy, ultrasound pachymetry, disc photography (Visucam Pro NM; Carl Zeiss Meditec, Inc., Dublin, CA), and visual field testing (Swedish Interactive Threshold Algorithm 24-2 test of the Humphrey visual field analyzer 750i, Carl Zeiss Meditec, Inc., Dublin, CA).

Patients were eligible to participate in the longitudinal SD-OCT Imaging Glaucoma study if they consented to the research OCT imaging protocol on the same day as their full eye examination, disc photography, and visual field testing. SD-OCT imaging was performed using the FDA approved Spectralis SD-OCT (Heidelberg Engineering GmbH, Heidelberg, Germany) with dilated pupils. Each eye underwent peripapillary RNFL thickness circular scans and optic nerve volume scans. The RNFL scan circle was 12 degrees in diameter, or approximately 3.5–3.6 mm in diameter for a typical eye length. The research imaging protocol included an optic nerve volume scan which was comprised of 193 raster B-scans. The field of view was a square region of 20×20 degrees, or approximately $6 \text{ mm} \times 6 \text{ mm}$. Automatic real-time function (ART) was enabled and set for three frames at each scan location.

All study patients had at least 4 annual follow-up visits with repeat dilated clinical exams, repeat routine clinical testing, and repeat high-density research optic nerve volume scans.

Definition of Open Angle Glaucoma with General Inclusion and Exclusion Criteria

Our study population consisted of patients with both primary and secondary open angle glaucomas (i.e. primary open angle, normal tension, pseudoexfoliation, and pigmentary). Primary open angle glaucoma (POAG) patients had disc and field changes with pre-treatment intraocular pressures (IOP) $> 21 \text{ mmHg}$; normal tension glaucoma (NTG) patients had disc and field changes with pre-treatment IOPs $\leq 21 \text{ mmHg}$; pseudoexfoliation

glaucoma (PXG) patients had pseudoexfoliative changes on slit lamp examination with disc and field changes; and pigmentary glaucoma (PDG) patients had pigmentary dispersion signs on slit lamp exam with disc and field changes.

Open angle glaucoma patients had characteristic optic nerve changes, corresponding visual field defects, and open-angles on gonioscopic examination. Glaucomatous optic nerve changes were defined based on criteria from the Ocular Hypertension Treatment Study (OHTS), which included characteristic rim thinning in a generalized or localized pattern while demonstrating 1 or more of the following characteristics: change in the position of the vessels greater than expected from a shift in the position of the eye, development of a notch, development of an acquired pit, and development of localized or diffuse pallor. Disc hemorrhage, nerve fiber layer dropout, and a deep cup change were not a requirement for glaucoma.¹⁶ Visual fields were considered abnormal if three or more contiguous test locations on one side of the horizontal meridian were depressed by 5 dB with at least 1 point depressed 10 dB from normative values.¹⁷ Glaucoma staging was based on the Hodapp-Anderson-Parrish system, with early stage glaucoma (mean deviation [MD] > -6 dB), moderate stage glaucoma (-12 dB < MD < -6 dB), or severe stage glaucoma (MD < -12 dB).

General inclusion criteria included patients with spherical equivalent between -6.0 and +6.0 diopters, best corrected visual acuity of 20/70 or better, clear visible disc photographs, and reliable visual field tests, which were defined as 33% fixation losses, 33% false-positive results, and 33% false-negative results.¹⁸ SD-OCT scans included in the study needed to meet the following criteria: signal strengths of 15 dB or more (range: 0-40), clear visibility of fundus images for RNFL thickness scans, and completion of 193 line raster scans for optic nerve volume scans.

Exclusion criteria included congenital abnormalities of the anterior chamber, corneal scarring or opacities, severe non-proliferative or proliferative diabetic retinopathy, visual field loss due to a non-glaucomatous condition or due to artifacts, or missing data. If both eyes of a patient were eligible for the study, one eye was selected using a random number generator through Microsoft excel 2013. The random number was generated using the function “=RANDBETWEEN(min,max),” where “min” was defined as “1” and “max” was defined as “2”. The value “1” was previously assigned to the “right eye” and the value of “2” was assigned to the “left eye.”

SD-OCT Data from RNFL Thickness Scans and Research Optic Nerve Volume Scans

The RNFL thickness was calculated by the Spectralis SD-OCT software (HRA/Spectralis software version 5.4.8.0). The RNFL thickness values were reported for global (360 degrees), for quadrants (i.e. inferior, superior, nasal, and temporal), and for sectors (i.e. inferior-nasal [IN], superior-nasal [SN], inferior-temporal [IT], and superior-temporal [ST]) values in an RNFL single exam report. From baseline RNFL thickness scans, artifacts were identified and classified according to the 12 artifact types as defined by the Liu et al study.¹⁰

The 3D optic nerve volume scan raw data were exported, and the custom-designed program calculated MDB thickness with C++ software developed at the Massachusetts Eye and

Ear using the Open Source libraries Insight Segmentation and Registration Toolkit (ITK version 4.3, Insight Software Consortium, Kitware Inc., Clifton Park, NY) and Open Source Computer Vision (OpenCV version 2.4.3; Willow Garage, Menlo Park, CA). The MDB thickness was calculated by building a 3D model of the RPE/BM complex, which was reconstructed from the individual B-scans. Processing of the SD-OCT volume scans was described in detail in a prior publication.¹³ All 193 B-scan images of each patient were checked for segmentation artifacts by one of the authors (K.R.). Segmentation artifacts that consisted of either misidentification or improper segmentation of the ILM and RPE were manually deleted, and the software was then used to recalculate the measurements. The disc margin, defined by the RPE/BM termination, was identified by 100 points spaced by 3.6 degrees. The central axis of the disc was determined by finding the centroid of the opening in the RPE/BM. For each angular interval of 3.6 degrees, the point on the disc margin closest to the disc axis was identified and the shortest distance from this point to the ILM was measured as the MDB thickness. MDB thickness values were determined for global (360 degrees), for 90-degree quadrants (i.e. inferior, superior, nasal, and temporal), and for 45 degree sectors (i.e. inferior-nasal [IN], superior-nasal [SN], inferior-temporal [IT], and superior-temporal [ST]).

Glaucoma Progression Analysis: Definition of Onset of Progression

Glaucoma progression analysis was determined separately for the disc photographs, visual fields, RNFL thickness assessments, and MDB thickness assessments using event-based analysis. The first date of the series for each modality showing progression was defined as the date of progression.

Determination of Disc Photography Progression

All disc photographs were de-identified by one of our authors (K.R.). Glaucoma progression status was independently determined by two glaucoma specialists (M.A.M. and C.L.O.) using disc photographs which were placed in a random order by one of our authors (J.K.). The 2 graders were blinded to all clinical and OCT data. The disc photography progression was determined if there was increased or new thinning of the optic nerve rim in a generalized or localized pattern that demonstrated specific characteristics as mentioned above. The evaluators received all disc photographs of each eye in a random order. Then they independently determined which disc photos showed glaucoma progression. Therefore, the evaluators had to both determine the order and at which time point or at which photo progression occurred. Any disagreement of the progression status between the two graders was resolved by a third glaucoma specialist (T.C.C.), until all 3 glaucoma specialists reached a unanimous determination of stable or progressed. Time to progression was determined by matching the disc photographs showing progression to the database of dates which the photos were taken.

Determination of Visual Field Progression

All visual fields were de-identified by one of our authors (K.R.). Glaucoma progression status was independently determined by two glaucoma specialists (M.A.M. and C.L.O.) using visual field analyses arranged by chronology. The 2 graders were blinded to all clinical and OCT data. The visual field progression was determined if at least one of

the following were present: deepening of an existing scotoma, expanding of an existing scotoma, and/or new localized visual field defect observed in a previously normal part of the field.^{8,17} Each grader viewed all visual fields for each eye and classified each eye as either stable or progressed by selecting the dates of the visual fields showing progression. Any disagreement of the progression status between the two graders was resolved by a third glaucoma specialist (T.C.C.), until all 3 glaucoma specialists reached a unanimous determination of stable or progressed.

Determination of SD-OCT Progression: RNFL Thinning and MDB Neuroretinal Rim Thinning

The RNFL thickness and MDB rim thickness were analyzed for glaucoma progression if serial measurements demonstrated a negative trend with decreased values larger than expected test-retest variability and mean normal aging changes. The same changes were also confirmed in the latest follow-up visit to avoid false predictive values. The false predictive values were defined when patients were initially determined as progressors due to significant decrease in measurement values, but then returned back to baseline in the follow-up visits. Based on previous literature, test-retest variability of RNFL thickness in global overall, inferior, and superior quadrants ranged from 2.65–3.89 μm , 3.89–7.20 μm , and 4.05–7.03 μm respectively.^{19–23} Rounding off to the nearest integer which may be seen on OCT printouts, the cut-off values for test-retest variability used in this study were 5, 8, and 8 μm for RNFL thickness in the global, inferior, and superior quadrants respectively. For MDB thickness, the test-retest variability in global overall ranged from 3.44–5.91 μm ,^{13,19} 3.40 μm for inferior,¹³ and 3.68 μm ¹³ for superior quadrants. The cut-off values for test-retest variability used in this study were 7, 5, and 5 μm for MDB thickness in the global, inferior, and superior quadrants respectively. Using past literature which reported on within-subject standard deviation (Sw), the values of test-retest variability were calculated using the formula $2 \times 1.645 \times \text{Sw}$.^{20,22} Based on previous literature, the normal rate of aging changes for RNFL thickness using Spectralis OCT were $-0.44 \mu\text{m}/\text{year}$ for global overall, $-0.37 \mu\text{m}/\text{y}$ for superior quadrant, and $-0.39 \mu\text{m}/\text{year}$ for inferior quadrant.²⁴ Tsikata et al reported the normal rate of aging changes for global MDB thickness as $-0.75 \mu\text{m}/\text{year}$,¹³ but there is no data for quadrants or sectors. For global overall and quadrants, the normal rates of aging changes used in this study were -0.5 and $-1.0 \mu\text{m}/\text{year}$ for RNFL thickness and MDB thickness respectively.^{13,24}

Statistical Analysis

Summary data were reported as means \pm standard deviation for continuous variables and as counts with percentages for categorical variables. The sample size calculation was done in 2010 when the longitudinal SD-OCT Imaging Glaucoma study was planned in our research group. At that time, the reproducibility of peripapillary RNFL thickness measurements using Spectralis OCT was determined to be up to 2.4 microns.²⁰ When assuming a standard deviation of 2.4 microns and a null change of 2.2 microns (aging effect) over 5 years, the sample size calculation revealed that 125 patients were needed for initial enrollment, in order to have at least 100 patients available for the analysis at 5 years, assuming an attrition rate of 20% over a 5-year follow-up. One hundred patients can detect a change of at least 2.88 microns over 5 years. Of the 2,000 study participants, only the first consecutive

124 patients who met inclusion and exclusion criteria were included for analysis. For comparisons between 2 groups, t-tests were used for continuous outcomes and Chi-square tests were used for categorical outcomes. McNemar's tests were performed to compare the number (percentage) of progressing eyes defined by the two modalities in paired fashion. Kaplan-Meier survival curves were constructed to analyze time-to-progression data. A robust variance procedure was used to account for the comparisons of paired progressions within each patient. Reported *P*-values from the log-rank test were adjusted for multiple comparisons using the Holm-Bonferroni method. Cohen's kappa coefficients were calculated to measure agreement of progressing eyes defined by the two modalities in paired fashion. All statistical analysis was performed using the statistical software R (version 3.3.3) and Stata (version 13.0). The threshold for statistical significance was defined as $P < 0.05$.

RESULTS

The first 133 consecutive open angle glaucoma patients were recruited for the study from the 2,000 subjects enrolled in the longitudinal SD-OCT Imaging Glaucoma study at Massachusetts Eye and Ear. Nine of 133 patients (6.8%) were excluded for the following reasons: 5 patients were missing at least one disc photograph or visual field test, 2 patients had incomplete volumetric scans, 1 patient had a possible non-glaucomatous visual field defect, and 1 patient exhibited algorithm failure. A total of 124 eyes from 124 included patients were analyzed in the final analysis (Table 1). About half the patients had POAG (67 patients, 54.0%), and about half had mild glaucoma (73 patients, 58.9%). Average longitudinal follow-up period was about 5 years (66.9 ± 16.4 months).

Table 2 shows the average baseline values for the OCT parameters: 2D RNFL thickness and 3D MDB neuroretinal rim thickness, or MDB thickness. RNFL thickness values ranged from 55 μm in the nasal quadrant to 85.7 μm in the supero-temporal sector, while the MDB thickness showed higher values ranging from 188 μm in the temporal quadrant to 234 μm in the supero-nasal sector.

Table 3 shows the number and percentage of eyes determined to exhibit glaucoma progression using event-based criterion for all 4 modalities i.e. disc photography, visual fields, RNFL thickness, and MDB neuroretinal rim thickness. Global MDB thickness showed glaucoma progression in the highest percentage of eyes compared to disc photography (52.4% versus 16.1%, $P < 0.001$) and global RNFL thickness measurements (52.4% versus 15.3%, $P < 0.001$). Regarding agreement of glaucoma progressing eyes for all 4 modalities in paired fashion, agreements were slight to fair as kappa values ranged from 0.095 to 0.300 (Table 4). The false predictive values when using OCT-based parameters were shown as 16 of 124 eyes (12.9%) by RNFL thickness progression and 31 of 124 eyes (25%) by MDB thickness progression.

Figure 1 depicts Kaplan-Meier survival curves, which were used to compare event-based analysis across all 4 modalities (disc photography, visual fields, global RNFL thickness, and global MDB rim thickness). Figure 1 demonstrates that the global MDB thickness detected progression significantly earlier than either disc photography or global RNFL thickness ($P < 0.001$). Table 5 shows the median time to progression (with 95% CI) for the subgroup of

patients who were determined to have progressed by each modality, and results indicate that global MDB neuroretinal rim thickness detected glaucoma progression approximately 1–2 years earlier than conventional testing (i.e. disc photograph and global RNFL thickness). Of the 65 of 124 eyes (52.4%) which were determined to have progressed by MDB thickness measurements, glaucoma progression for 30 of these 65 eyes (46.2%) was simultaneously (15 eyes; 23.1%) or later (15 eyes; 23.1%) confirmed by other conventional modalities (i.e. DP, VF, and 2D RNFL thickness measurements). Figure 2 shows an example of longitudinal changes with progressive MDB thinning, as shown by 3D pictorial outputs created from the customized software developed at Massachusetts Eye and Ear.

Kaplan-Meier survival curves compared global values, inferior quadrants, and superior quadrants for MDB thickness (Figure 3) and RNFL thickness (Figure 4), and these figures demonstrated that there were no statistically significant differences in glaucoma progression detection between global, inferior, and superior regions for MDB thickness ($P = 0.33\text{--}0.67$) and for RNFL thickness ($P = 0.06\text{--}0.74$).

DISCUSSION

Over a 5-year period, high-density 3D OCT neuroretinal rim measurements (i.e. MDB thickness) detected glaucoma progression in a higher percentage of eyes (52.4%) compared to traditional modalities, such as disc photography (16.1%, $P < 0.001$) and 2D global RNFL thickness measurements (15.3%, $P < 0.001$; Table 3). To our knowledge, this is the first study comparing commonly used clinical modalities (disc photography, visual fields, and 2D OCT RNFL thickness) for their abilities to detect event-based glaucoma progression versus the new 3D OCT neuroretinal rim parameter, which maximizes 3D SD-OCT's imaging potential for quantifying neuroretinal rim tissue.

3D OCT neuroretinal rim measurements can detect glaucoma progression almost 2 years earlier than disc photography ($P < 0.001$, Figure 1, Table 5). Over an average of 5 years, disc photography detected glaucoma progression in 16.1% of eyes (Table 3), which is similar to prior studies^{25,26}; however, the global MDB rim thickness measurement detected glaucoma progression in a higher percentage of eyes at 52.4% ($P < 0.001$, Table 3). This suggests that SD-OCT MDB rim thickness measurements are possibly more sensitive than disc photography (Table 3), although the agreement of detecting glaucoma progressing eyes determined by MDB rim thickness measurements and disc photography was slight ($k=0.110$, Table 4). The slight agreement between the tests may partly be attributed to the fact that glaucoma progression by MDB thickness is objective while glaucoma progression by disc photography is subjective, and there is theoretically more variability for subjective assessments. Plus, MDB thickness and disc photography assessments are measuring different neuroretinal rim locations (i.e. MDB neuroretinal rim is the shortest distance between the RPE/BMO complex and the ILM and is quantified in 3D space, versus disc photography neuroretinal rim is visualized in a horizontal plane). This is consistent with other OCT studies, which have also suggested that SD-OCT RNFL thickness measurements can detect glaucoma progression better than disc photography.^{21,27} Specifically, Wessel et al showed that glaucoma progression by SD-OCT RNFL thickness measurements was detected in 60% of non-progressing eyes as defined by optic disc assessments.²¹ Lee

et al also showed that SD-OCT RNFL thickness measurements were more sensitive in detecting diffuse loss compared to disc photography assessments.²⁷ In addition to being more sensitive, SD-OCT MDB neuroretinal rim thickness measurements have the added advantages of being both objective and quantitative versus the subjective and qualitative data afford by disc photography. It is conceptually difficult to conceive that disc photography could detect the small micron changes of the neuroretinal rim which can be detected by a SD-OCT-based parameter. Additionally, disc photography classically exhibits moderate to poor agreement between specialist observers.^{4-6,26}

High-density 3D OCT neuroretinal rim measurements are more sensitive in detecting glaucoma progression compared to RNFL thickness measurements (Tables 3 and 5, Figure 1). However, the agreement of detecting structural progression among OCT-based measurements and disc photography was slight to fair ($k=0.095-0.300$, Table 4). The values of agreement among conventional tests and OCT tests were low (Table 4), possibly because of different algorithms, different machines, and different areas measured for these 4 modalities. Although this is the only longitudinal study which compares high-density MDB neuroretinal rim measurements versus RNFL thickness measurements, there is a prior study comparing the relationship between low-density BMO-MRW neuroretinal rim thickness and RNFL thickness, and that study contradicted the results we found in our study.²⁸ In that prior study, Gardiner et al reported that RNFL thickness was able to detect longitudinal change better than the low-density BMO-MRW (P value = 0.025).²⁸ The differences between the current study and the Gardiner et al study may be attributable to the possibility that high-density rim parameters (i.e. MDB thickness) are more sensitive than RNFL thickness, while low-density rim parameters (i.e. BMO-MRW) are not. Other differences in our study compared to prior studies were that our study found a lower percentage of progressing eyes using RNFL thickness compared to most previous studies (i.e. 13.7–25.8% in our study [Table 3] versus 24.7–62.2% in previous studies).²⁹⁻³¹ Those differing percentages may be attributable to different criteria in defining glaucoma progression.

In addition to having a higher density scan protocol, there are many other reasons that MDB rim thickness detected glaucoma progression in a higher percentage of eyes and earlier than RNFL thickness. First, the dynamic range of MDB rim thickness is greater with a smaller floor effect than RNFL thickness. From our study (Table 2) and from previous MDB studies, glaucoma patients had an average thickness of approximately 150 to 250 μm for MDB thickness and 50 to 90 μm for RNFL thickness.^{12,13} A study of rhesus monkeys further showed that the MDB is composed primarily of nerve tissue, with 94% of the neuroretinal rim consisting of ganglion cell nerve axons (i.e. potential dynamic range) and 5% of the rim consisting of astrocytes (i.e. potential floor effect).³² Therefore, the measurement floor of non-neuronal tissue for MDB thickness could be around 12–18 μm for normal subjects.^{12,13} In contrast to MDB thickness, RNFL thickness has a measurement floor of non-neuronal tissue of around 49.2–64.7 μm , which may include glial cells and vascular tissue as measured by three commonly used OCT devices i.e. Spectralis, Cirrus, and RTVue.⁹ The greater dynamic range with smaller floor effect of MDB thickness potentially leads to earlier detection of smaller changes compared to RNFL thickness. Secondly, MDB thickness is easier to measure more accurately and reliably in glaucoma patients compared to RNFL

thickness. Specifically, the borders of the MDB, which is delimited by the RPE/BMO and ILM, are highly reflective in OCT images. In contrast, the posterior boundary of the RNFL is more difficult to determine with glaucoma, because RNFL reflectivity decreases with glaucoma. This loss of RNFL reflectivity makes it more difficult to differentiate the normally highly reflective RNFL from the underlying less reflective ganglion cell layer.¹⁴ Thirdly, the MDB is probably damaged earlier in glaucomatous eyes than the RNFL. He et al found that in experimental glaucomatous monkey eyes, MRW changed earlier than RNFL thickness; and that Kaplan-Meier curves were significantly better for MRW compared to RNFL thickness for both event-based ($P=0.049$) and trend-based criteria ($P=0.019$), respectively.³³ Lastly, MDB thickness measurements derived from a volume scan may have fewer clinically significant artifacts than with RNFL thickness. For this study, B-scans used for MDB thickness calculations were manually reviewed and frames with artifacts were discarded before the calculations done, but discarded frames could be compensated for by interpolation of data from neighboring frames, thus still enabling accurate MDB thickness calculations. In contrast, we found that up to 45 of 124 patients (36.3%) of baseline RNFL thickness scans contained artifacts, most of which were from incorrect segmentation of the posterior RNFL layer and from a decentered scan. These artifacts may affect the reproducibility and accuracy of RNFL thickness measurements,^{2,34} because sometimes repeat RNFL scanning is needed to correct for these errors. All these explanations would account for the ability of MDB thickness to detect earlier smaller changes in glaucoma patients compared to RNFL thickness.

There was no significant difference in percentage of glaucoma progressed eyes defined between 3D OCT neuroretinal rim measurements and visual field testing (52.4% versus 43.5%, $P=0.124$; Table 3). Although 43.5% of our study patients progressed by visual field testing (Table 3), this rate was similar to some previous studies^{25,35–37} but higher compared to other studies (12.1–31%).^{31,38–42} Our findings may differ from previous studies, because we had a different study design, a different study population, and a different method of defining visual field progression. Despite our study consisting mainly of mild glaucoma patients (73 patients, 58.9%, [Table 1]), OCT-based MDB thickness progression occurred in a similar percentage of eyes compared to visual field progression (52.4% versus 43.5%, $P=0.124$). Our finding was different than previous studies which found that both time domain OCT⁴³ and SD-OCT^{2,29,31,44–46} were more effective than visual fields at detecting glaucoma progression especially in early stage glaucoma. These other studies also support the general concept that structural glaucoma progression precedes functional damage.^{47–53} However, when glaucoma progression occurs, structural damage may occur first, functional damage may occur first, or both can progress simultaneously. Therefore, it is not surprising that agreement between MDB thickness and visual fields for detecting glaucoma progression was slight ($k=0.183$, Table 4). Other reasons for slight agreement between MDB neuroretinal thickness and visual fields were that OCT progression was objectively determined and visual fields were subjectively assessed. The algorithms and definitions of glaucoma progression were also different between the tests. In theory, visual fields may be worse than OCT structural measurements for detecting progression, because visual fields have more test-retest variability and less repeatability than OCT measurements.⁵⁴ Plus, Heijl et al showed that test-retest variability was higher in glaucoma

patients compared to normal subjects, especially in the area of a field defect.⁵⁴ Poor visual field repeatability was also demonstrated by the Ocular Hypertension Treatment Study, which suggested that 86% of visual field defects were not reproducible on repeat testing.⁷

In 3D OCT neuroretinal rim measurements, average or overall MDB thickness is a sensitive parameter for glaucoma progression detection. From our study, there was no statistically significant differences among regions of interests in OCT-based glaucoma progression detection (Figure 3 for MDB thickness, Figure 4 for RNFL thickness). Our findings are similar to a previous study where Danthurebandara et al showed that BMO-MRW and RNFL thickness sectoral analysis was equivalent to total analysis for detecting glaucomatous change.⁵⁵ However, Danthurebandara's study and the current study contrasts with most of the past literature, which suggests longitudinal differences among regions of interest in OCT scans.^{21,56-62} For example, Jonas suggested that the inferior and superior regions were vulnerable for glaucomatous damage due to the large pore area in the lamina cribosa.⁶³ Wessel et al similarly reported that the inferior sector showed the highest degree of nerve loss in glaucoma progressing eyes compared to non-progressing eyes.²¹ Diniz-Filho et al also reported the largest differences in OCT change between progressing and non-progressing eyes in the superior and inferior regions.⁵⁶ Our results may differ from others studies, because the high-density MDB thickness measurement may be more sensitive than the traditional RNFL thickness measurement for detecting small changes even in global measurements and not just quadrant or sector measurements. The 3D MDB rim thickness measurement has an automated disc centration feature and is therefore is less prone to de-centration errors. In contrast, RNFL thickness quadrant measurements (i.e. superior, nasal, inferior, temporal) are more susceptible to de-centration artifacts than global average RNFL thickness measurements.³⁴ Although our results showed that RNFL thickness measurements for global, superior, and inferior regions were statistically similar for the detection of glaucoma progression, there was a trend for inferior RNFL thickness perhaps detecting glaucoma earlier than global overall and superior quadrant regions ($P=0.09$ between global overall and inferior quadrant, $P=0.06$ between inferior and superior quadrant).

There were some limitations in our study. First, the results of our study may not be generalizable if different definitions of glaucoma progression were used, if different patient populations were studied, such as those with poor vision or high myopia, or if different cutoff-values of event-based glaucoma progression and rates of aging change were used. Because there are no exact values of test-retest variability and of age-related change for MDB and RNFL thickness measurements, we determined a range for these values based on a literature search. If studies were to use different test-retest variability values or use different age-related change values, study results may differ. Second, our study design did not include a repeat test on the same day, or within a short period of time, to confirm progression. Repeat confirmation testing may help to reduce the rate of false positives and false negatives.^{7,8,40} In our study, we found a small but significant rate of false predictive values when using OCT-based parameters [i.e. 16 of 124 eyes (12.9%) by RNFL progression and 31 of 124 eyes (25%) by MDB progression]. Although these patients were not included in the final count of progressors, this shows that false predictive values may occur in a real clinical setting and can lead to an initial overestimation of glaucoma progression. Because false predictive values were noted for both MDB thickness measurements and

for RNFL thickness, a repeat OCT test to confirm glaucoma progression is recommended. Third, the recorded time of glaucoma progression might be delayed with annual follow-up testing. Chauhan et al showed that visual field testing performed once a year detected field progression approximately 3 years later than if testing were performed three times per year in patients with rapid progression.³ The time period would be delayed even more in the groups of patients with moderate and slow visual field progression.³ Fourth, without a commonly accepted gold standard test for detecting glaucoma progression, each modality might include both true positives and false positives. Therefore, combining tests to determine progression of disease is recommended. Lastly, there was no subgroup analysis based on severity of disease. Our study mainly consisted of mild glaucoma patients (73 patients, 58.9%, Table 1). In contrast, moderate to advanced glaucoma patients may have higher test-retest variability, and the floor effect would more likely play a greater role in limiting the ability to detect OCT progression in these advanced glaucoma patients.⁹ The ability to detect progression among the various modalities may vary depending on the severity of disease.^{43,44}

In conclusion, the high-density 3D neuroretinal rim parameter (i.e. MDB thickness) maximizes the full potential of SD-OCT for glaucoma imaging and shows superiority over disc photography and 2D RNFL thickness measurements for detecting glaucoma progression approximately 1–2 years earlier by event-based analysis. These findings show that the high-density MDB neuroretinal rim thickness measurement is a promising objective quantitative tool for determining structural progression in glaucoma.

ACKNOWLEDGEMENTS & DISCLOSURES

Financial Support:

Teresa C. Chen: Harvard Catalyst Grant (National Institutes of Health Award UL1 RR 025758, Bethesda, Maryland), Massachusetts Lions Eye Research Fund (New Bedford, Boston, Massachusetts), American Glaucoma Society Mid-Career Award (San Francisco, California), Fidelity Charitable Fund (Harvard University, Boston, Massachusetts), Department of Defense Small Business Innovation Research DHP15-016. Johannes F. de Boer: Dutch Science foundation, HealthHolland, Heidelberg Engineering. The funding sources had no role in the study design or conduct of this research.

Financial Disclosures:

Johannes F. de Boer: Sponsored research Heidelberg Engineering, GmbH, Germany; Licenses to NIDEK Inc., Fremont, CA; Terumo Corporation, Tokyo, Japan; Ninepoint Medical, Cambridge, MA; and Heidelberg Engineering, GmbH, Germany. The remaining authors declare no conflict of interest.

Other Acknowledgements:

None

REFERENCES

1. Vianna JR, Chauhan BC. How to detect progression in glaucoma. *Prog Brain Res*. 2015;221:135–158. [PubMed: 26518076]
2. Tatham AJ, Medeiros FA. Detecting structural progression in glaucoma with optical coherence tomography. *Ophthalmology*. 2017;124(12S):S57–S65. [PubMed: 29157363]
3. Chauhan BC, Garway-Heath DF, Goni FJ, et al. Practical recommendations for measuring rates of visual field change in glaucoma. *Br J Ophthalmol*. 2008;92(4):569–573. [PubMed: 18211935]

4. Jampel HD, Friedman D, Quigley H, et al. Agreement among glaucoma specialists in assessing progressive disc changes from photographs in open-angle glaucoma patients. *Am J Ophthalmol.* 2009;147(1):39–44.e31. [PubMed: 18790472]
5. Coleman AL, Sommer A, Enger C, Knopf HL, Stamper RL, Minckler DS. Interobserver and intraobserver variability in the detection of glaucomatous progression of the optic disc. *J Glaucoma.* 1996;5(6):384–389. [PubMed: 8946294]
6. Abrams LS, Scott IU, Spaeth GL, Quigley HA, Varma R. Agreement among optometrists, ophthalmologists, and residents in evaluating the optic disc for glaucoma. *Ophthalmology.* 1994;101(10):1662–1667. [PubMed: 7936564]
7. Keltner JL, Johnson CA, Quigg JM, Cello KE, Kass MA, Gordon MO. Confirmation of visual field abnormalities in the Ocular Hypertension Treatment Study. Ocular Hypertension Treatment Study Group. *Arch Ophthalmol.* 2000;118(9):1187–1194. [PubMed: 10980763]
8. Schulzer M Errors in the diagnosis of visual field progression in normal-tension glaucoma. *Ophthalmology.* 1994;101(9):1589–1594; discussion 1595. [PubMed: 8090461]
9. Mwanza JC, Kim HY, Budenz DL, et al. Residual and dynamic range of retinal nerve fiber layer thickness in glaucoma: Comparison of three OCT platforms. *Invest Ophthalmol Vis Sci.* 2015;56(11):6344–6351. [PubMed: 26436887]
10. Liu Y, Simavli H, Que CJ, et al. Patient characteristics associated with artifacts in Spectralis optical coherence tomography imaging of the retinal nerve fiber layer in glaucoma. *Am J Ophthalmol.* 2015;159(3):565–76.e2. [PubMed: 25498118]
11. Fan KC, Tsikata E, Khoueir Z, et al. Enhanced diagnostic capability for glaucoma of 3-dimensional versus 2-dimensional neuroretinal rim parameters using spectral domain optical coherence tomography. *J Glaucoma.* 2017;26(5):450–458. [PubMed: 28234677]
12. Shieh E, Lee R, Que C, et al. Diagnostic performance of a novel three-dimensional neuroretinal rim parameter for glaucoma using high-density volume scans. *Am J Ophthalmol.* 2016;169:168–178. [PubMed: 27349414]
13. Tsikata E, Lee R, Shieh E, et al. Comprehensive three-dimensional analysis of the neuroretinal rim in glaucoma using high-density spectral-domain optical coherence tomography volume scans. *Invest Ophthalmol Vis Sci.* 2016;57(13):5498–5508. [PubMed: 27768203]
14. Chen TC. Spectral domain optical coherence tomography in glaucoma: qualitative and quantitative analysis of the optic nerve head and retinal nerve fiber layer (an AOS thesis). *Trans Am Ophthalmol Soc.* 2009;107:254–281. [PubMed: 20126502]
15. Staurengi G, Sadda S, Chakravarthy U, Spaide RF. Proposed lexicon for anatomic landmarks in normal posterior segment spectral-domain optical coherence tomography: the IN*OCT consensus. *Ophthalmology.* 2014;121(8):1572–1578. [PubMed: 24755005]
16. Gordon MO, Kass MA. The Ocular Hypertension Treatment Study: design and baseline description of the participants. *Arch Ophthalmol.* 1999;117(5):573–583. [PubMed: 10326953]
17. Comparison of glaucomatous progression between untreated patients with normal-tension glaucoma and patients with therapeutically reduced intraocular pressures. Collaborative Normal-Tension Glaucoma Study Group. *Am J Ophthalmol.* 1998;126(4):487–497. [PubMed: 9780093]
18. Johnson CA, Keltner JL, Cello KE, et al. Baseline visual field characteristics in the Ocular Hypertension Treatment Study. *Ophthalmology.* 2002;109(3):432–437. [PubMed: 11874743]
19. Reis ASC, Zangalli CES, Abe RY, et al. Intra- and interobserver reproducibility of Bruch's membrane opening minimum rim width measurements with spectral domain optical coherence tomography. *Acta Ophthalmol.* 2017;95(7):e548–e555. [PubMed: 28650590]
20. Wu H, de Boer JF, Chen TC. Reproducibility of retinal nerve fiber layer thickness measurements using spectral domain optical coherence tomography. *J Glaucoma.* 2011;20(8):470–476. [PubMed: 20852437]
21. Wessel JM, Horn FK, Tornow RP, et al. Longitudinal analysis of progression in glaucoma using spectral-domain optical coherence tomography. *Invest Ophthalmol Vis Sci.* 2013;54(5):3613–3620. [PubMed: 23633657]
22. Mwanza JC, Chang RT, Budenz DL, et al. Reproducibility of peripapillary retinal nerve fiber layer thickness and optic nerve head parameters measured with cirrus HD-OCT in glaucomatous eyes. *Invest Ophthalmol Vis Sci.* 2010;51(11):5724–5730. [PubMed: 20574014]

23. Lee SH, Kim SH, Kim TW, Park KH, Kim DM. Reproducibility of retinal nerve fiber thickness measurements using the test-retest function of spectral OCT/SLO in normal and glaucomatous eyes. *J Glaucoma*. 2010;19(9):637–642. [PubMed: 20173650]
24. Bowd C, Zangwill LM, Weinreb RN, et al. Racial differences in rate of change of spectral-domain optical coherence tomography-measured minimum rim width and retinal nerve fiber layer thickness. *Am J Ophthalmol*. 2018;196:154–164. [PubMed: 30195890]
25. Ohnell H, Heijl A, Brenner L, Anderson H, Bengtsson B. Structural and functional progression in the Early Manifest Glaucoma Trial. *Ophthalmology*. 2016;123(6):1173–1180. [PubMed: 26949119]
26. Saarela V, Falck A, Airaksinen PJ, Tuulonen A. The sensitivity and specificity of Heidelberg Retina Tomograph parameters to glaucomatous progression in disc photographs. *Br J Ophthalmol*. 2010;94(1):68–73. [PubMed: 19692360]
27. Lee JR, Sung KR, Na JH, Shon K, Lee KS. Discrepancy between optic disc and nerve fiber layer assessment and optical coherence tomography in detecting glaucomatous progression. *Jpn J Ophthalmol*. 2013;57(6):546–552. [PubMed: 24097099]
28. Gardiner SK, Boey PY, Yang H, Fortune B, Burgoyne CF, Demirel S. Structural measurements for monitoring change in glaucoma: Comparing retinal nerve fiber layer thickness with minimum rim width and area. *Invest Ophthalmol Vis Sci*. 2015;56(11):6886–6891. [PubMed: 26501416]
29. Zhang X, Dastiridou A, Francis BA, et al. Comparison of glaucoma progression detection by optical coherence tomography and visual field. *Am J Ophthalmol*. 2017;184:63–74. [PubMed: 28964806]
30. Hou HW, Lin C, Leung CK. Integrating macular ganglion cell inner plexiform layer and parapapillary retinal nerve fiber layer measurements to detect glaucoma progression. *Ophthalmology*. 2018;125(6):822–831. [PubMed: 29433852]
31. Yu M, Lin C, Weinreb RN, Lai G, Chiu V, Leung CK. Risk of visual field progression in glaucoma patients with progressive retinal nerve fiber layer thinning: A 5-year prospective study. *Ophthalmology*. 2016;123(6):1201–1210. [PubMed: 27001534]
32. Minckler DS, McLean IW, Tso MO. Distribution of axonal and glial elements in the rhesus optic nerve head studied by electron microscopy. *Am J Ophthalmol*. 1976;82(2):179–187. [PubMed: 821348]
33. He L, Yang H, Gardiner SK, et al. Longitudinal detection of optic nerve head changes by spectral domain optical coherence tomography in early experimental glaucoma. *Invest Ophthalmol Vis Sci*. 2014;55(1):574–586. [PubMed: 24255047]
34. Cheung CY, Yiu CK, Weinreb RN, et al. Effects of scan circle displacement in optical coherence tomography retinal nerve fibre layer thickness measurement: a RNFL modelling study. *Eye (Lond)*. 2009;23(6):1436–1441. [PubMed: 18806767]
35. Heijl A, Leske MC, Bengtsson B, Hyman L, Bengtsson B, Hussein M. Reduction of intraocular pressure and glaucoma progression: results from the Early Manifest Glaucoma Trial. *Arch Ophthalmol*. 2002;120(10):1268–1279. [PubMed: 12365904]
36. Gros-Otero J, Castejon M, Paz-Moreno J, Mikropoulos D, Teus M. Perimetric progression using the Visual Field Index and the Advanced Glaucoma Intervention Study score and its clinical correlations. *J Optom*. 2015;8(4):232–238. [PubMed: 25182851]
37. Ohnell H, Heijl A, Anderson H, Bengtsson B. Detection of glaucoma progression by perimetry and optic disc photography at different stages of the disease: results from the Early Manifest Glaucoma Trial. *Acta Ophthalmol*. 2017;95(3):281–287. [PubMed: 27778463]
38. The effectiveness of intraocular pressure reduction in the treatment of normal-tension glaucoma. Collaborative Normal-Tension Glaucoma Study Group. *Am J Ophthalmol*. 1998;126(4):498–505. [PubMed: 9780094]
39. Musch DC, Gillespie BW, Lichter PR, Niziol LM, Janz NK. Visual field progression in the Collaborative Initial Glaucoma Treatment Study the impact of treatment and other baseline factors. *Ophthalmology*. 2009;116(2):200–207. [PubMed: 19019444]
40. Kim J, Dally LG, Ederer F, et al. The Advanced Glaucoma Intervention Study (AGIS): 14. Distinguishing progression of glaucoma from visual field fluctuations. *Ophthalmology*. 2004;111(11):2109–2116. [PubMed: 15522379]

41. Nouri-Mahdavi K, Caprioli J, Coleman AL, Hoffman D, Gaasterland D. Pointwise linear regression for evaluation of visual field outcomes and comparison with the Advanced Glaucoma Intervention Study methods. *Arch Ophthalmol*. 2005;123(2):193–199. [PubMed: 15710815]
42. Anton A, Pazos M, Martin B, et al. Glaucoma progression detection: agreement, sensitivity, and specificity of expert visual field evaluation, event analysis, and trend analysis. *Eur J Ophthalmol*. 2013;23(2):187–195. [PubMed: 23065852]
43. Kaushik S, Mulkutkar S, Pandav SS, Verma N, Gupta A. Comparison of event-based analysis of glaucoma progression assessed subjectively on visual fields and retinal nerve fiber layer attenuation measured by optical coherence tomography. *Int Ophthalmol*. 2015;35(1):95–106. [PubMed: 25502985]
44. Tenkumo K, Hirooka K, Baba T, Nitta E, Sato S, Shiraga F. Evaluation of relationship between retinal nerve fiber layer thickness progression and visual field progression in patients with glaucoma. *Jpn J Ophthalmol*. 2013;57(5):451–456. [PubMed: 23797700]
45. Abe RY, Diniz-Filho A, Zangwill LM, et al. The relative odds of progressing by structural and functional tests in glaucoma. *Invest Ophthalmol Vis Sci*. 2016;57(9):OCT421–OCT428. [PubMed: 27409501]
46. Banegas SA, Anton A, Morilla A, et al. Evaluation of the retinal nerve fiber layer thickness, the mean deviation, and the visual field index in progressive glaucoma. *J Glaucoma*. 2016;25(3):e229–e235. [PubMed: 26020689]
47. Chauhan BC, Nicolela MT, Artes PH. Incidence and rates of visual field progression after longitudinally measured optic disc change in glaucoma. *Ophthalmology*. 2009;116(11):2110–2118. [PubMed: 19500850]
48. Leung CK, Yu M, Weinreb RN, Lai G, Xu G, Lam DS. Retinal nerve fiber layer imaging with spectral-domain optical coherence tomography: patterns of retinal nerve fiber layer progression. *Ophthalmology*. 2012;119(9):1858–1866. [PubMed: 22677426]
49. Sommer A, Katz J, Quigley HA, et al. Clinically detectable nerve fiber atrophy precedes the onset of glaucomatous field loss. *Arch Ophthalmol*. 1991;109(1):77–83. [PubMed: 1987954]
50. Harwerth RS, Carter-Dawson L, Shen F, Smith EL 3rd, Crawford ML. Ganglion cell losses underlying visual field defects from experimental glaucoma. *Invest Ophthalmol Vis Sci*. 1999;40(10):2242–2250. [PubMed: 10476789]
51. Kerrigan-Baumrind LA, Quigley HA, Pease ME, Kerrigan DF, Mitchell RS. Number of ganglion cells in glaucoma eyes compared with threshold visual field tests in the same persons. *Invest Ophthalmol Vis Sci*. 2000;41(3):741–748. [PubMed: 10711689]
52. Quigley HA, Addicks EM, Green WR. Optic nerve damage in human glaucoma. III. Quantitative correlation of nerve fiber loss and visual field defect in glaucoma, ischemic neuropathy, papilledema, and toxic neuropathy. *Arch Ophthalmol*. 1982;100(1):135–146. [PubMed: 7055464]
53. De Moraes CG, Liebmann JM, Park SC, et al. Optic disc progression and rates of visual field change in treated glaucoma. *Acta Ophthalmol*. 2013;91(2):e86–91. [PubMed: 23356423]
54. Heijl A, Lindgren A, Lindgren G. Test-retest variability in glaucomatous visual fields. *Am J Ophthalmol*. 1989;108(2):130–135. [PubMed: 2757094]
55. Danthurebandara VM, Vianna JR, Sharpe GP, et al. Diagnostic accuracy of glaucoma with sector-based and a new total profile-based analysis of neuroretinal rim and retinal nerve fiber layer thickness. *Invest Ophthalmol Vis Sci*. 2016;57(1):181–187. [PubMed: 26795824]
56. Diniz-Filho A, Abe RY, Zangwill LM, et al. Association between intraocular pressure and rates of retinal nerve fiber layer loss measured by optical coherence tomography. *Ophthalmology*. 2016;123(10):2058–2065. [PubMed: 27554036]
57. Leung CK, Yu M, Weinreb RN, et al. Retinal nerve fiber layer imaging with spectral-domain optical coherence tomography: a prospective analysis of age-related loss. *Ophthalmology*. 2012;119(4):731–737. [PubMed: 22264886]
58. Schrems WA, Mardin CY, Horn FK, Juenemann AG, Laemmer R. Comparison of scanning laser polarimetry and optical coherence tomography in quantitative retinal nerve fiber assessment. *J Glaucoma*. 2010;19(2):83–94. [PubMed: 19373100]

59. Suda K, Hangai M, Akagi T, et al. Comparison of longitudinal changes in functional and structural measures for evaluating progression of glaucomatous optic neuropathy. *Invest Ophthalmol Vis Sci*. 2015;56(9):5477–5484. [PubMed: 26284553]
60. Thenappan A, De Moraes CG, Wang DL, et al. Optical coherence tomography and glaucoma progression: A comparison of a region of interest approach to average retinal nerve fiber layer thickness. *J Glaucoma*. 2017;26(5):473–477. [PubMed: 28263263]
61. Leung CK, Cheung CY, Weinreb RN, et al. Evaluation of retinal nerve fiber layer progression in glaucoma: a study on optical coherence tomography guided progression analysis. *Invest Ophthalmol Vis Sci*. 2010;51(1):217–222. [PubMed: 19684001]
62. Lee EJ, Kim TW, Weinreb RN, Park KH, Kim SH, Kim DM. Trend-based analysis of retinal nerve fiber layer thickness measured by optical coherence tomography in eyes with localized nerve fiber layer defects. *Invest Ophthalmol Vis Sci*. 2011;52(2):1138–1144. [PubMed: 21051691]
63. Jonas JB, Mardin CY, Schlotzer-Schrehardt U, Naumann GO. Morphometry of the human lamina cribrosa surface. *Invest Ophthalmol Vis Sci*. 1991;32(2):401–405. [PubMed: 1993592]

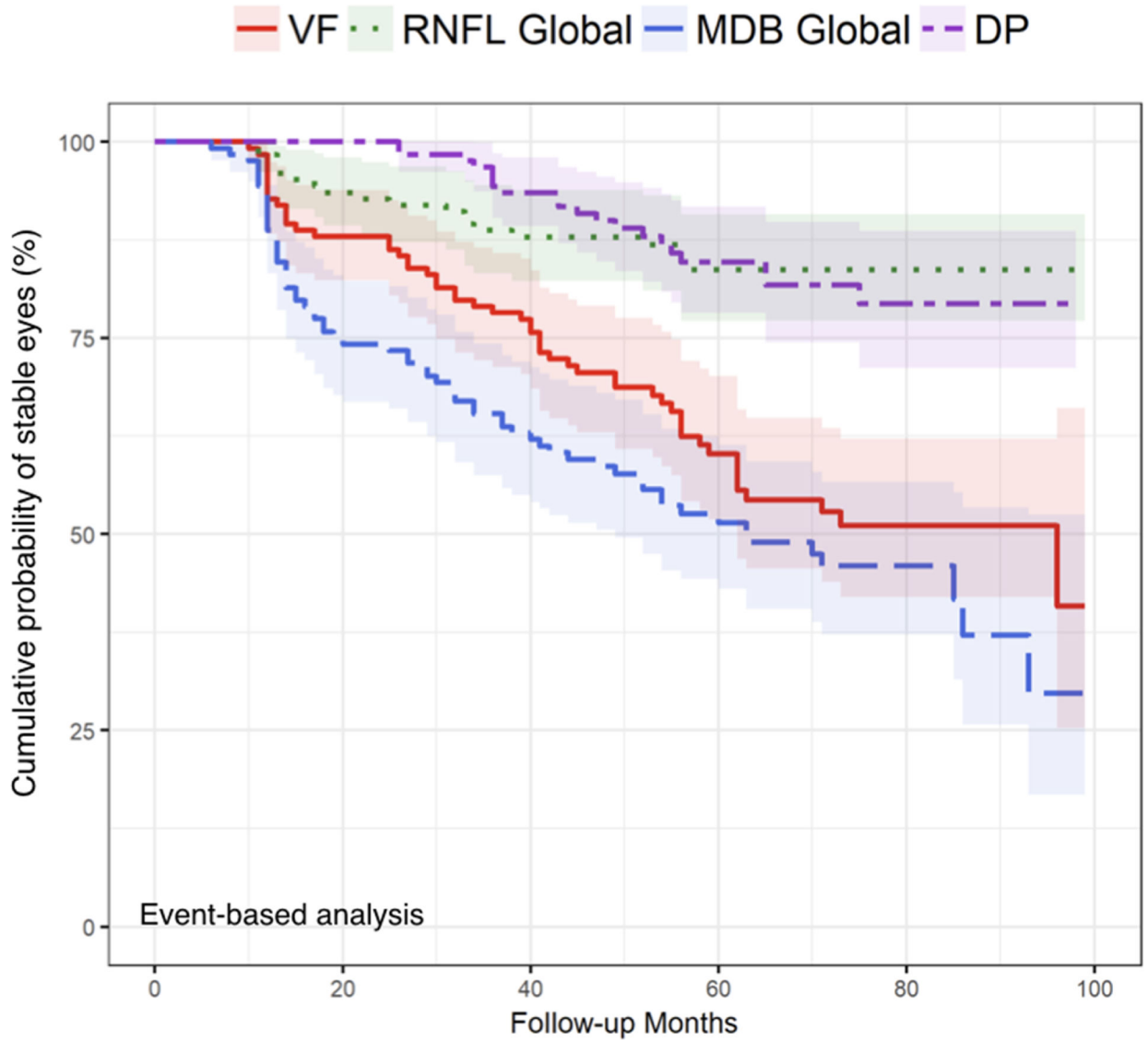


FIGURE 1. Comparison of event-based analysis Kaplan-Meier curves across visual field (VF), global two-dimensional retinal nerve fiber layer (RNFL) thickness, global three-dimensional neuroretinal rim thickness [minimum distance band (MDB) thickness], and disc photograph (DP). Log-rank tests were used to compare the global MDB thickness method to VF, global RNFL thickness, and DP with $P = 0.15$, < 0.001 , and < 0.001 respectively, indicating that global MDB thickness by event-based criterion detected progression significantly earlier than global RNFL thickness and DP. The Holm method was used to adjust the log-rank tests for multiple comparisons.

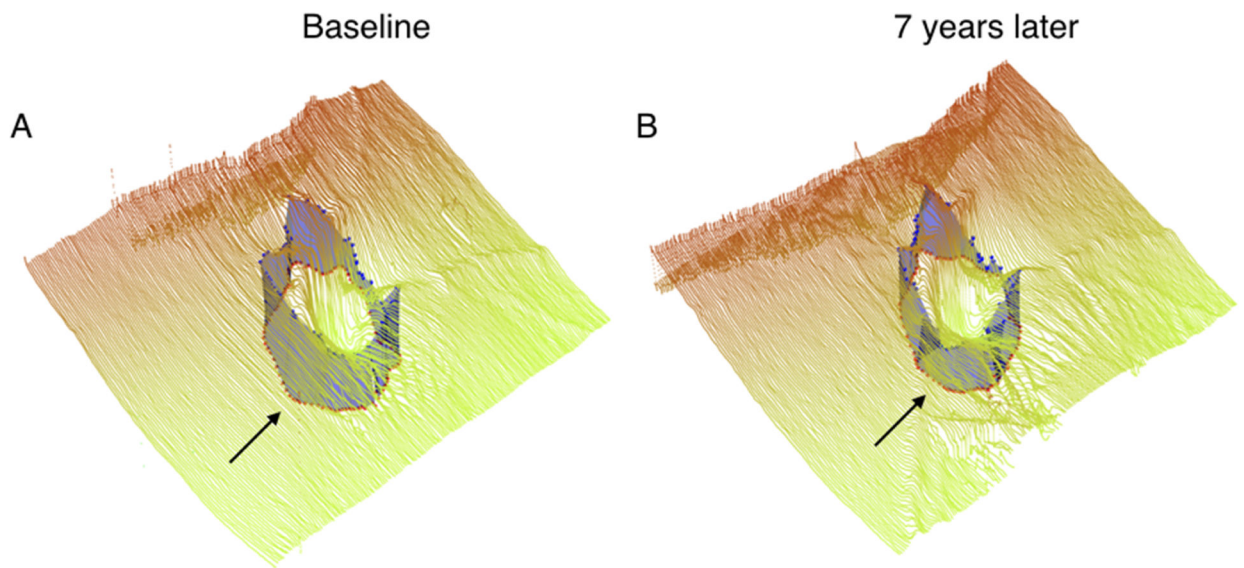


FIGURE 2.

Example of the three-dimensional neuroretinal rim thickness [minimum distance band (MDB)] of a progressing left eye imaged with Spectralis spectral-domain optical coherence tomography. (A) Baseline global MDB thickness of the left eye (B) Global MDB thickness of the left eye 7 years later.

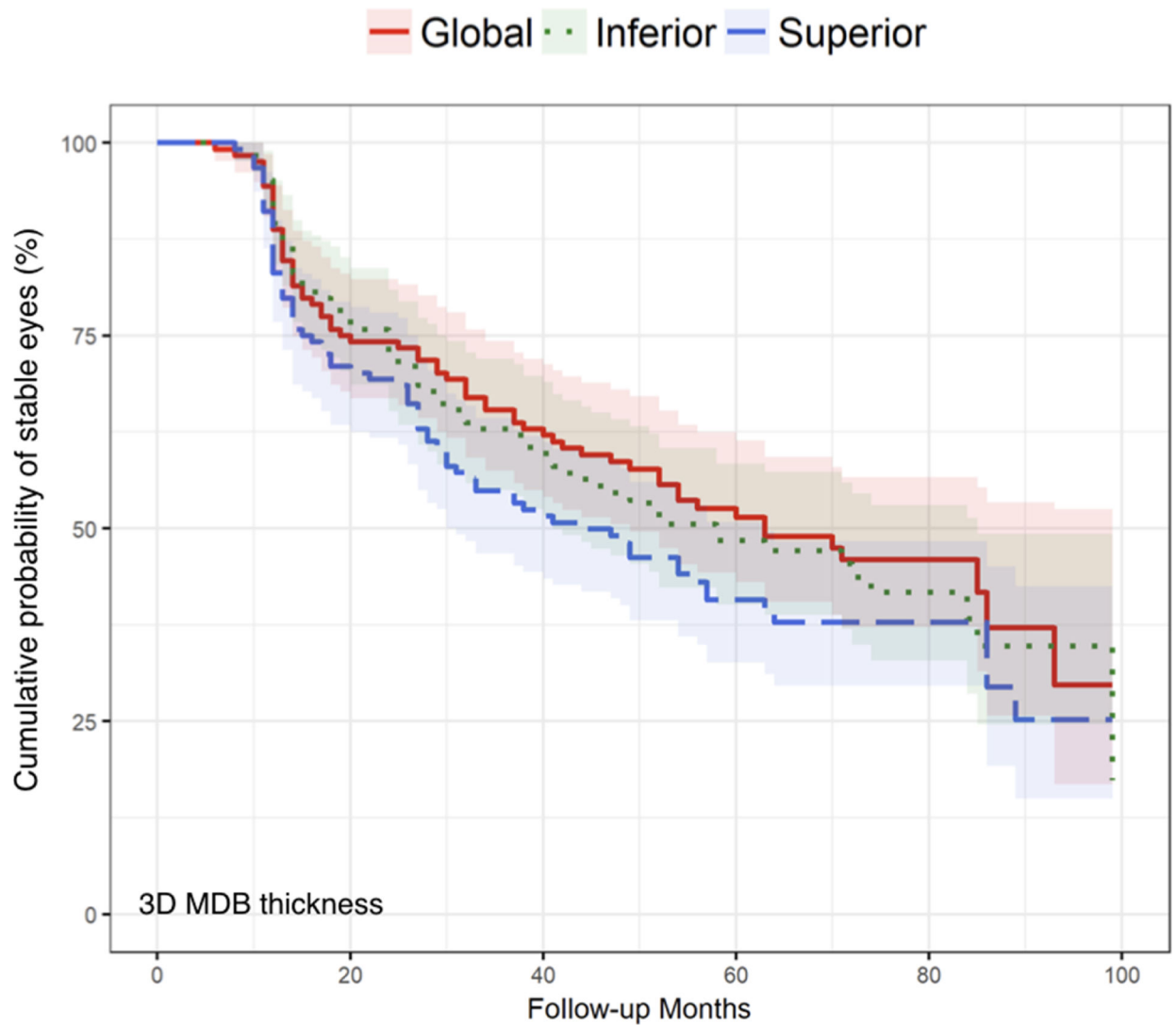


FIGURE 3.

Comparison of event-based analysis Kaplan-Meier curves of three-dimensional minimum distance band (MDB) thickness measurement across global overall, inferior, and superior quadrants methods. Log-rank tests were used to compare the global MDB thickness method to the inferior quadrant and superior quadrant methods, with $P = 0.67$ and $P = 0.33$ respectively. Additionally, for the comparison between the inferior quadrant and superior quadrant, $P = 0.48$, indicating that there is no significant difference among the three methods in detecting glaucoma progression using event-based criterion. The Holm method was used to adjust the log-rank tests for multiple comparisons.

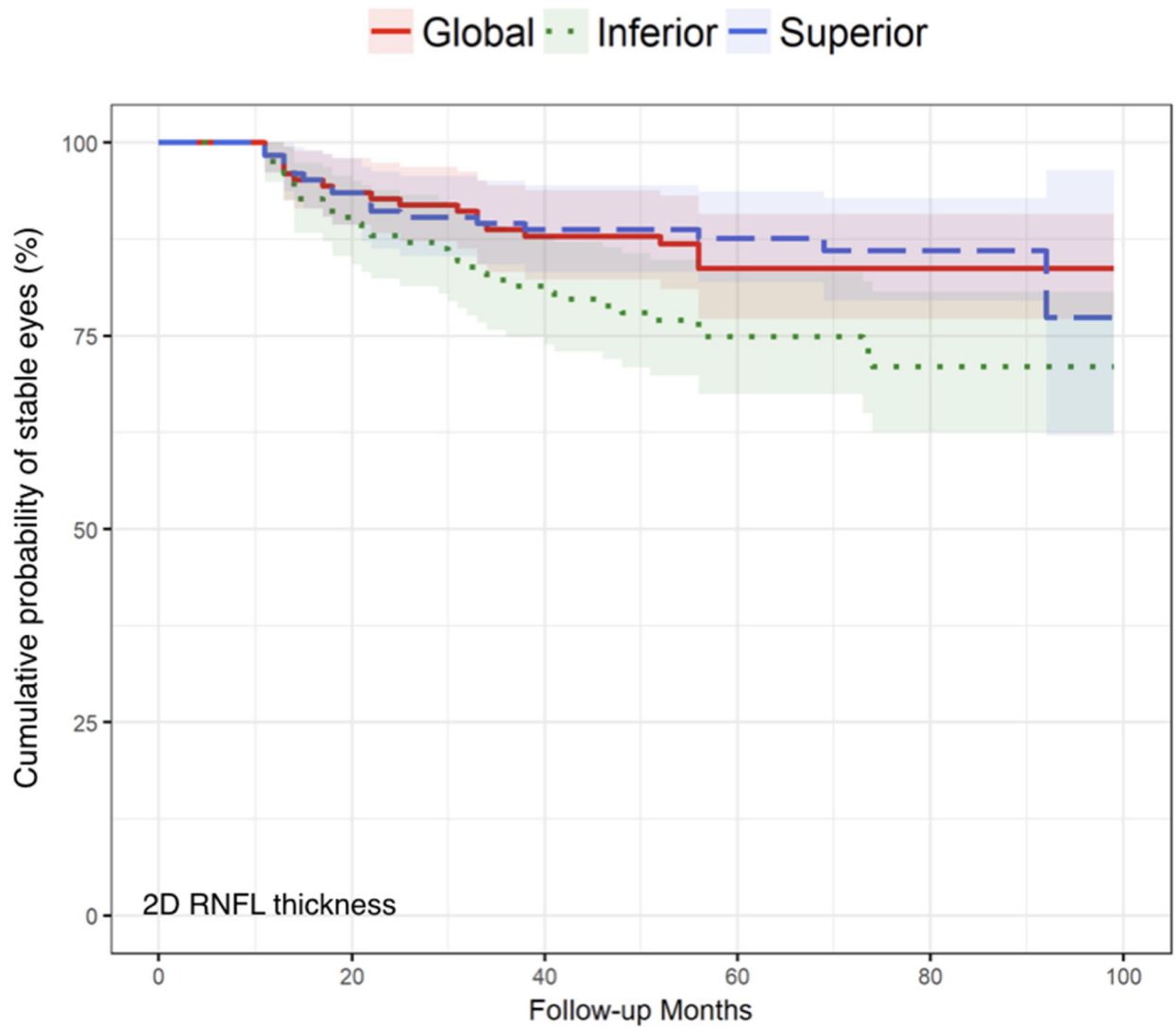


FIGURE 4.

Comparison of event-based analysis Kaplan-Meier curves of two-dimensional retinal nerve fiber layer (RNFL) thickness measurement across global overall, inferior, and superior quadrants methods. Log-rank tests were used to compare the global RNFL thickness method to the inferior quadrant and superior quadrant methods, with $P = 0.09$ and $P = 0.74$ respectively. Additionally, for the comparison between the inferior quadrant and superior quadrant, $P = 0.06$, indicating that there is no significant difference among the three methods in detecting glaucoma progression using event-based criterion. The Holm method was used to adjust the log-rank tests for multiple comparisons.

TABLE 1.**Baseline Demographic and Clinical Characteristics of Open-Angle Glaucoma Study Patients**

Characteristics	Study Cohort (124 Patients)
Number of eyes	124
Number of right eyes/left eyes (%)	63 (50.8%) / 61 (49.2%)
Age, year (mean \pm SD)	68.1 \pm 11.6
Female, <i>n</i> (%)	62 (50.0%)
Race, <i>n</i> (%)	
Caucasian	91 (73.4%)
African-American	19 (15.3%)
Asian	8 (6.5%)
Hispanic	3 (2.4%)
Other	3 (2.4%)
Family history of glaucoma in 1 st degree relative, <i>n</i> (%)	36 (29.0%)
Type of glaucoma, <i>n</i> (%)	
Primary open-angle glaucoma	67 (54.0%)
Normal-tension glaucoma	21 (16.9%)
Pseudoexfoliative glaucoma	24 (19.4%)
Pigmentary glaucoma	12 (9.7%)
Severity of glaucoma ^a , <i>n</i> (%)	
Mild (MD > -6 dB)	73 (58.9%)
Moderate (-12 dB < MD \leq -6 dB)	29 (23.4%)
Severe (MD \leq -12 dB)	22 (17.7%)
Spherical equivalent, diopters (mean \pm SD)	-0.9 \pm 2.1
Intraocular pressure, mmHg (mean \pm SD)	15.2 \pm 4.7
Central corneal thickness, μ m (mean \pm SD)	539.4 \pm 38.1
Vertical cup-to-disc ratio (mean \pm SD)	0.6 \pm 0.2
Visual field (mean \pm SD)	
Mean deviation, dB	-6.9 \pm 6.3
Pattern standard deviation, dB	5.5 \pm 3.6
Number of visits (mean \pm SD)	5.2 \pm 1.1
Follow-up period, months (mean \pm SD)	66.9 \pm 16.4

The data was reported as mean \pm standard deviation (SD) for continuous variables and frequency count (%) for categorical variables.

^aSeverity of glaucoma was classified based on visual field mean deviation (MD).

TABLE 2.

Baseline Spectral-Domain Optical Coherence Tomography Diagnostic Parameters of Open-Angle Glaucoma Study Patients

Region of Interest	2D RNFL thickness	3D neuroretinal rim thickness
Global overall, μm (mean \pm SD)	67.4 \pm 16.2	213.3 \pm 55.7
Quadrant, μm (mean \pm SD)		
Inferior	78.5 \pm 25.5	214.9 \pm 72.8
Superior	79.4 \pm 23.2	223.2 \pm 74.7
Nasal	55.0 \pm 19.6	227.3 \pm 72.9
Temporal	57.5 \pm 14.8	188.0 \pm 64.9
Sector, μm (mean \pm SD)		
Infero-nasal	74.4 \pm 26.9	233.0 \pm 79.8
Supero-nasal	73.2 \pm 24.0	234.0 \pm 83.4
Infero-temporal	82.7 \pm 32.9	196.7 \pm 78.7
Supero-temporal	85.7 \pm 28.8	218.3 \pm 74.1

2D indicates two-dimensional; 3D, three-dimensional; RNFL, retinal nerve fiber layer. The data was reported as mean \pm standard deviation (SD) for continuous variables.

TABLE 3.

Number and Percentage of Eyes Exhibiting Glaucoma Progression by Event-based Criterion for Disc Photograph, Visual Field, Two-Dimensional Retinal Nerve Fiber Layer Thickness, and Three-Dimensional Neuroretinal Rim Thickness

Modality	Progression detection by event-based criterion	<i>P</i> -values ^a
Disc photograph, <i>n</i> (%)	20 (16.1%)	< 0.001 *
Visual field, <i>n</i> (%)	54 (43.5%)	0.124
2D RNFL thickness, <i>n</i> (%)		
Global overall	19 (15.3%)	< 0.001 *
3D neuroretinal rim thickness, <i>n</i> (%)		
Global overall	65 (52.4%)	-

2D indicates two-dimensional; 3D, three-dimensional; RNFL, retinal nerve fiber layer.

^a*P*-values obtained using McNemar's test for comparing the number of progressing eyes defined by between 3D neuroretinal rim thickness and other modalities i.e. disc photograph, visual field, and 2D RNFL thickness measurements in paired fashion.

* Statistically significant *P*-value < .05

TABLE 4.

Agreement of Glaucoma Progression by Event-Based Criteria for Disc Photography, Visual Fields, Two-Dimensional Retinal Nerve Fiber Layer Thickness, and Three-Dimensional Neuroretinal Rim Thickness

Modality	Disc Photography	Visual Fields	2D RNFL thickness	3D neuroretinal rim thickness
Disc Photography		0.187	0.300	0.110
Visual Fields			0.167	0.183
2D RNFL thickness				0.095
3D neuroretinal rim thickness				

2D = two-dimensional; 3D = three-dimensional; RNFL = retinal nerve fiber layer. *Paired fashion using Cohen's kappa coefficients*

TABLE 5.

Median Time to Glaucoma Progression for the Subgroup of Patients who Progressed According to the Event-based Criterion for Each Modality using Kaplan-Meier Survival Analysis.

Modality	Median time to event-based progression (months; 95%CI)
Disc photograph	44 (36, 55)
Visual field	32 (27, 41)
2D RNFL thickness	
Global overall	33 (31, -) [†]
3D neuroretinal rim thickness	
Global overall	23 (17, 32)

CI indicates confidence interval; 2D, two-dimensional; 3D, three-dimensional; RNFL, retinal nerve fiber layer.

[†] indicates that the number of eyes meeting the progression criteria for this modality was too low to compute the upper limit of the 95% CI.